Near-threshold vibrational excitation of H_2 by positron impact: A projection-operator approach

Márcio T. do N. Varella and Marco A. P. Lima
Instituto de Física Gleb Wataghin, Universidade Estadual de Campinas, UNICAMP, 13083-970 Campinas, São Paulo, Brazil
(Received 29 November 2006; published 6 November 2007)

We report vibrational excitation ($\nu_i=0 \rightarrow \nu_f=1$) and total cross sections for positron scattering by H_2. The Feshbach projection operator formalism was employed to vibrationally resolve the fixed-nuclei phase shifts obtained with the Schwinger multichannel method. The near-threshold behavior of the vibrational excitation cross section is in good agreement with available experimental data [Sullivan *et al.*, Phys. Rev. Lett. **86**, 1494 (2001)]. Though our fixed-nuclei calculations do not indicate the existence of a e^+-H_2 virtual state, a proper description of the T matrix threshold behavior is essential (the adiabatic approximation is inadequate). The projection operator approach has long been a powerful tool for studies of nuclear dynamics in electron-molecule collisions, and its application to positron scattering is timely since couplings to nuclear degrees of freedom are known to be very important at low impact energies.

DOI: 10.1103/PhysRevA.76.052701 PACS number(s): 34.85.+x, 34.10.+x, 34.50.Ez, 34.50.Pi

I. INTRODUCTION

The recent improvements in positron accumulation and beam techniques [1–3] allowed for a new generation of scattering [4–9] and annihilation [10–12] experiments that greatly expanded the understanding of positron-matter interactions in the gas phase. In particular, the evidence of vibrationally enhanced annihilation [10–12] and vibrationally resolved cross sections [4,9] have attracted a lot of attention to the couplings between positron and nuclear degrees of freedom. Though considerable insight into the role of vibrations has been gained from phenomenological [13–15] and analytically solvable [16] models since a mechanism based on vibrational resonances [17,18] was proposed to explain the very large annihilation rates of polyatomics [10–12,18–20], *ab initio* descriptions of realistic systems would also contribute to build up a sound theoretical understanding.

Though Gianturco and co-workers have been undertaking an effort in this direction [21–29], the literature on vibrational excitation of molecules by positron impact is sketchy. Our group has investigated the dependence of the e^+-acetylene compound energy on C-C stretch [30] and carried out a comparative study of (adiabatic) vibrational excitation of hydrogen by electron and positron impact [31,32], but so far our studies have essentially focused on fixed-nuclei elastic collisions [30,33–39] and electronic excitation [40,41]. In this work, we present a formulation based on the Feshbach projection-operator formalism [42] that may allow for systematic studies of vibration dynamics in positron scattering.

The projection-operator formalism has long been known a powerful technique for studies of nuclear dynamics in electron scattering, and a review of the vast literature on applications to electron-molecule resonances, virtual, and bound states is out of the scope of this work. We only mention a review article [43] and a few recent applications [44,45] (the reader is referred to other papers in Sec. II). This essentially exact formalism decomposes the scattering wave function in two components, namely the discrete state and the background continuum, where the former is embedded and coupled to the latter. The collision is described as the formation of a transient projectile-target state that launches the nuclei onto a complex and energy-dependent potential surface arising from the discrete-continuum coupling, and long-lived transients significantly release energy into the nuclear degrees of freedom. The formalism provides a suitable strategy for vibrational resolution of fixed-nuclei cross sections, and its application to positron collisions is timely in view of the recent interest on vibrational couplings.

The outline of this paper is as follows. In Sec. II we briefly present our approach to fixed-nuclei scattering (Schwinger Multichannel method), discuss the main features of the vibrational excitation formulation and a computational implementation that allows for a proper description of the s wave dependence on the positron energy and nuclear coordinates. The s wave is dominant at low energies and is expected to account for the relevant dynamics of near-threshold collisions. We present vibrationally resolved cross sections for hydrogen in Sec. IV and our conclusions are presented in Sec. V.

II. THEORY

The Hamiltonian for positron-molecule collisions is given by

$$H = K + H_{\text{ele}} = K + H_0 + V, \tag{1}$$

where K is the nuclear kinetic energy operator, V is the positron-molecule scattering potential, and H_0 is the electronic interaction-free Hamiltonian, i.e., the sum of the positron kinetic energy and the N-electron target Hamiltonian,

$$H_0 = -\frac{1}{2}\nabla_{\text{p}}^2 + H_N, \tag{2}$$

with the nuclear repulsion included in the latter. For simplicity, we restrict the formulation to a single vibrational mode and a single energy-allowed electronic channel (the target ground state). The T matrix element for the $\nu_i \rightarrow \nu_f$ vibrational excitation is given by

$$T_{\nu_f,\nu_i}(\mathbf{k}_f,\mathbf{k}_i) = \langle \Phi_{\mathbf{k}_f\nu_f}|V|\Psi^{(+)}_{\mathbf{k}_i\nu_i}\rangle = \langle \Phi_{\mathbf{k}_f\nu_f}|T|\Phi_{\mathbf{k}_i\nu_i}\rangle, \quad (3)$$

where $\mathbf{k}_i$ and $\mathbf{k}_f$ are the incoming and outgoing positron wave vectors, respectively, $|\Phi_{\mathbf{k}\nu}\rangle$ is an asymptotic (interaction-free) state and $|\Psi^{(+)}_{\mathbf{k}_i\nu_i}\rangle$ is the scattering wave function (an eigenstate of H).

Assuming the validity of the Born-Oppenheimer (BO) approximation [46] for the target, the free states may be written as

$$\Phi_{\mathbf{k}\nu}(\mathbf{R},\mathbf{r}_p,\rho) = N(k)\exp(i\mathbf{k}\cdot\mathbf{r}_p)\phi_0(\mathbf{R};\rho)\eta_\nu(\rho), \quad (4)$$

where $N(k)$ is a normalization factor, ρ is the vibrational coordinate, $\mathbf{r}_p$ are the positron coordinates, $\mathbf{R}=\{\mathbf{r}_1,\ldots,\mathbf{r}_N\}$ stands for the coordinates of N target electrons, ϕ_0 and η_ν are electronic and vibrational target eigenstates, respectively, and the semicolon $(;\rho)$ denotes parametric dependence on ρ. The vibrational Hamiltonian of the target is given by

$$\tilde{H}_N = K + \langle\phi_0|H_N|\phi_0\rangle \equiv K + V_0(\rho), \quad (5)$$

with

$$\tilde{H}_N|\eta_\nu\rangle = \varepsilon_\nu|\eta_\nu\rangle. \quad (6)$$

Equation (4) is computationally convenient since BO ground states are routinely calculated with standard quantum chemical techniques, and this simple form can be extended to the scattering state through the adiabatic nuclei vibration (ANV) approximation [47]. The collision is assumed very fast in the time scale of nuclear motion, and vibration excitation thus takes place in the (N-electron) potential energy surface of the target, i.e.,

$$\Psi^{(+)}_{\mathbf{k}_i\nu_i}(\mathbf{R},\mathbf{r}_p,\rho) = \psi^{(+)}_{\mathbf{k}_i}(\mathbf{R},\mathbf{r}_p;\rho)\eta_{\nu_i}(\rho), \quad (7)$$

and

$$T_{\nu_f,\nu_i}(\mathbf{k}_f,\mathbf{k}_i) = \langle\eta_{\nu_f}|t(\mathbf{k}_f,\mathbf{k}_i;\rho)|\eta_{\nu_i}\rangle, \quad (8)$$

with

$$t(\mathbf{k}_f,\mathbf{k}_i;\rho) = \langle S_{\mathbf{k}_f}|V|\psi^{(+)}_{\mathbf{k}_i}\rangle. \quad (9)$$

$S_{\mathbf{k}_f}$ is an electronic free state (the product of a plane wave and the target electronic state), $\psi^{(+)}_{\mathbf{k}_i}$ is the fixed-nuclei scattering wave function, and integration over nuclear and electron (positron) coordinates is implied in Eqs. (8) and (9), respectively. In practice, Eq. (8) can be integrated on a quadrature by solving the fixed-nuclei scattering problem for the set of quadrature points.

Though the simplicity of the ANV framework is appealing, the underlying approximation breaks down when (i) the collision is long-lived (in case resonances, bound or virtual states are found), since appreciable nuclear motion takes place in the $(N+1)$-particle potential surface of the positron-target compound; and (ii) threshold effects are important, since Eq. (8) violates Wigner threshold law [48] ($k_i=k_f$ in the fixed-nuclei transition matrix element). In the following sections, we outline our approach to the fixed-nuclei scattering problem and how it can be combined with the projection operator formalism to overcome the limitations of the ANV approximation.

A. Fixed-nuclei scattering

We employ the Schwinger multichannel method (SMC) to solve the fixed-nuclei collision problem. The method is described in detail elsewhere [49] and here we only give the working expression for the transition matrix,

$$t(\mathbf{k}_f,\mathbf{k}_i) = \sum_{m,n}\langle S_{\mathbf{k}_f}|V|\chi_m\rangle(d^{-1})_{mn}\langle\chi_n|V|S_{\mathbf{k}_i}\rangle, \quad (10)$$

where

$$d_{mn} = \langle\chi_m|(PVP + Q\hat{H}_{ele}Q - VG^{(+)}_P V)|\chi_n\rangle. \quad (11)$$

The $(N+1)$-particle configuration state functions χ_m (products of target electronic states and positron scattering orbitals) provide a basis for expansion of the trial scattering wave function; P and $Q=(1-P)$ are projection operators onto open and closed target electronic channels, respectively; $G^{(+)}_P$ is the free-particle Green's function projected onto P space; and $\hat{H}_{ele}=(E-H_{ele})$, where E is the incident positron energy.

B. Projection-operator formalism

The Feshbach projection operator formalism [42] decomposes the scattering wave function into discrete ("resonant") and background components. Generalizations of the formalism to incorporate nuclear motion have long been proposed [50–55] and rely on a BO electronic discrete state [56]—in the present context, an $(N+1)$-particle state including the positron, $\phi_d(\mathbf{R},\mathbf{r}_p;\rho)$—that uniquely defines the projectors $\mathcal{Q}=|\phi_d\rangle\langle\phi_d|$ and $\mathcal{P}=(1-\mathcal{Q})$. Consequently,

$$\mathcal{Q}\mathcal{P} = \mathcal{P}\mathcal{Q} = [K,\mathcal{Q}] = [K,\mathcal{P}] = 0, \quad (12)$$

so the coupling between the discrete component ($\mathcal{Q}$ space) and the background continuum ($\mathcal{P}$ space) arises from the electronic Hamiltonian, $\mathcal{Q}H\mathcal{P}=\mathcal{Q}H_{ele}\mathcal{P}$. The formalism has been discussed by several authors (see, for instance, Refs. [51,55,57]), and only a few key aspects will be outlined here. The decomposition of the scattering wave function, $(\mathcal{P}+\mathcal{Q})|\Psi^{(+)}_{\mathbf{k}_i\nu_i}\rangle = |\Psi^{\mathcal{P}}_{\mathbf{k}_i\nu_i}\rangle + |\Psi^{\mathcal{Q}}_{\mathbf{k}_i\nu_i}\rangle$, leads to a two-potential problem [58] and ultimately splits up the T matrix [42,51,57] according to

$$T_{\nu_f,\nu_i}(\mathbf{k}_f,\mathbf{k}_i) = \langle\eta_{\nu_f}|t_{bg}(\mathbf{k}_f,\mathbf{k}_i;\rho)|\eta_{\nu_i}\rangle + \left\langle \eta_{\nu_f}\left| U^*_{\mathbf{k}_f}\frac{1}{E-K-V_{opt}(E-\tilde{H}_N)}U_{\mathbf{k}_i}\right|\eta_{\nu_i}\right\rangle. \quad (13)$$

The first term on the right-hand side (rhs) of Eq. (13) accounts for $\mathcal{P}$-space (background) scattering, and its calculation is straightforward [59]. In the second term on the rhs,

$$U_{\mathbf{k}}(\rho) = \langle\phi_d|H_{ele}|\phi^{\mathcal{P}}_{\mathbf{k}}\rangle \quad (14)$$

accounts for the electronic discrete-continuum ($\mathcal{Q}$-$\mathcal{P}$) coupling, where $U_{\mathbf{k}_i}$ and $U_{\mathbf{k}_f}$ are usually called entry and exit amplitudes [55], respectively. The optical potential is given by [57]

$$V_{\rm opt}(E-\tilde{H}_N) = V_0(\rho) + \epsilon_{\rm d}(\rho) + \Delta(E-\tilde{H}_N) - \frac{i}{2}\Gamma(E-\tilde{H}_N), \tag{15}$$

where

$$\epsilon_{\rm d}(\rho) = \langle \phi_{\rm d}|H_{\rm ele}|\phi_{\rm d}\rangle - V_0(\rho) \tag{16}$$

is the relative energy of the discrete state with respect to the electronic ground state of the target. Δ and Γ are the real and imaginary parts, respectively, of a complex, nonlocal, and energy-dependent potential arising from the coupling of the discrete state ($\phi_{\rm d}$) to the continuum of background scattering states. The width Γ is related to the discrete-continuum decay probability and the level shift Δ contributes to the real part of the optical potential surface ($V_0+\epsilon_{\rm d}+\Delta$). Explicitly [57],

$$\Gamma(E-\tilde{H}_N) = 2\pi \int kdk \int d\hat{\mathbf{k}} U_{\mathbf{k}} \delta\left(E-\tilde{H}_N-\frac{k^2}{2}\right) U_{\mathbf{k}}^*, \tag{17}$$

and

$$\Delta(E-\tilde{H}_N) = \frac{1}{2\pi} p \int dE' \frac{\Gamma(E'-\tilde{H}_N)}{E-E'-\tilde{H}_N}, \tag{18}$$

where the Cauchy principal value is indicated in Eq. (18).

Though the projection-operator formalism is not restricted to the description of resonant collisions, the first and second T matrix terms on the rhs of Eq. (13) are usually called background and resonant components, respectively, because many applications to electron-molecule shape resonances have been carried out. The approach is completely general in the sense that a decomposition of the wave function can always be performed, and it is likewise applicable to the description of bound and virtual states, or even to direct scattering (large $\mathcal{Q}$-$\mathcal{P}$ couplings give rise to short-lived collisions). Since no shape resonances are found in positron-molecule scattering, the broadly employed terminology "resonant component" would be misleading in the present case, and we employ "discrete component" instead. The underlying dynamical picture in Eq. (13) is the formation of a discrete state ($\phi_{\rm d}$), embedded and coupled to a background continuum, that launches a stationary vibrational eigenstate of the target (η_{ν_i}) onto the complex and energy dependent potential surface $V_{\rm opt}$. The discrete state eventually decays to the continuum by positron detachment, leaving the target in the vibrationally excited state η_{ν_f}.

The vibrational excitation integral cross section may be readily obtained from Eq. (13),

$$\sigma_{\nu_i\to\nu_f} = \frac{(2\pi)^3}{E}\left|\left\langle \eta_{\nu_f}\left| U_{E_f}\frac{1}{E-K-V_{\rm opt}(E-\tilde{H}_N)}U_E\right|\eta_{\nu_i}\right\rangle\right|^2, \tag{19}$$

where

$$|U_E|^2 = \int d\hat{\mathbf{k}}|U_{\mathbf{k}}|^2. \tag{20}$$

In Eq. (19), we set $\varepsilon_i=0$ by suitably choosing the zero of the target potential energy surface and $E=E_f+\varepsilon_f$ is the positron energy. The free asymptotic states were normalized as $N(k)=\sqrt{k/(2\pi)^3}$ [61], and the background contribution was omitted for simplicity ($t_{\rm bg}$ is weakly dependent on the nuclear coordinate by construction, $\langle \eta_{\nu_f}|t_{\rm bg}|\eta_{\nu_i}\rangle \simeq 0$, though it may contribute to vibrationally elastic scattering).

1. Fixed-nuclei input

Though the matrix element in Eq. (19) can be numerically integrated by solving the fixed-nuclei problem on the quadrature points once $\phi_{\rm d}(\mathbf{R},\mathbf{r}_p;\rho)$ is known, the discrete state is still to be determined. Several methods have been proposed for *ab initio* estimates of $\phi_{\rm d}$, such as Siegert-state [62], stabilization [63], Stieltjes-trajectory [64], complex-absorbing-potential [65], and R-matrix [66] techniques, but so far none has become a widely employed approach. The complex potential parameters are often obtained from standard scattering methods by fitting a Breit-Wigner profile [58] to cross sections or eigenphases [45,55,57,67,68].

It is known from formal scattering theory [69,70] that the decomposition of the fixed-nuclei T matrix is equivalent to the decomposition of the fixed-nuclei eigenphase sum,

$$\delta(E) = \delta_{\rm bg}(E) + \delta_{\rm d}(E), \tag{21}$$

with

$$\delta_{\rm d}(E) = -\tan^{-1}\left(\frac{(1/2)\Gamma(E)}{E-\epsilon_{\rm d}-\Delta(E)}\right). \tag{22}$$

An insightful way of obtaining the fixed-nuclei complex potential ($\epsilon_{\rm d},\Gamma,\Delta$) from *ab initio* eigenphases, proposed by Domcke and co-workers [57,67], assumes a model form for the energy dependence of the width. Though the formulation can be extended to higher angular momenta [57], we restrict ourselves to the s wave ($l=0$) and employ the simple parametrization

$$\Gamma(E) = AE^{1/2}\exp(-bE) \tag{23}$$

that incorporates the Wigner threshold law [48]. This model was originally applied to the e^--CO_2 virtual state [67], and considerably simplifies the projection-operator framework because the energy dependence of the complex potential is obtained in closed form. The level shift is obtained as [57]

$$\Delta(E) = \frac{A}{2}\left[\frac{-1}{\sqrt{\pi b}} + E^{1/2}e^{-bE}|\mathrm{erf}(i\sqrt{bE})|\right], \tag{24}$$

where erf is the error function [71]. The background eigenphase is given by the leading term of the threshold expansion,

$$\delta_{\rm bg}(E) = aE^{1/2}, \tag{25}$$

and the discrete state energy $\epsilon_{\rm d}$ is viewed as a model parameter, so the fixed-nuclei T matrix can be expressed in terms of a (background component), A, b, and $\epsilon_{\rm d}$ (complex poten-

tial). These model parameters may be readily obtained, for any given value of the vibrational coordinate, from a least-squares fit of Eq. (21) to SMC phase shifts, since $\delta(E)$ may be expressed in terms of $\{a,A,b,\epsilon_d\}$ upon substitution of Eqs. (22)–(25).

2. Implementation

The vibrational eigenstates of the target provide a convenient basis for representation of the complex and nonlocal operator in Eqs. (13) and (19),

$$\sum_{\nu}^{\oplus} |\eta_\nu\rangle\langle\eta_\nu| = 1, \tag{26}$$

where the contribution from continuum states should be negligible, since we are interested in near-threshold excitation to low-lying vibrational levels, and dissociative positron attachment would not be expected. From Eqs. (17) and (20), we have

$$\langle\eta_i|\Gamma(E-\tilde{H}_N)|\eta_j\rangle = 2\pi\sum_{\nu}\langle\eta_i|U_{E-\varepsilon_\nu}|\eta_\nu\rangle\langle\eta_\nu|U^*_{E-\varepsilon_\nu}|\eta_j\rangle, \tag{27}$$

and the neglect of an unimportant phase factor [72] leads to

$$\Gamma_{ij}(E) = \sum_{\nu}\langle\eta_i|\Gamma^{1/2}(E-\varepsilon_\nu)|\eta_\nu\rangle\langle\eta_\nu|\Gamma^{1/2}(E-\varepsilon_\nu)|\eta_j\rangle, \tag{28}$$

where $\Gamma_{ij}(E)$ is the matrix element of $\Gamma(E-\tilde{H}_N)$ and $\Gamma(E)$, given by Eq. (23), is now a parametric function of the vibrational coordinate: by performing least-squares fits of Eq. (21) to fixed-nuclei SMC phase shifts, as described above, the model parameters $\{a,A,b,\epsilon_d\}$ can be obtained on a set of quadrature points, and thus be viewed as functions of the vibrational coordinate. The width $\Gamma(E)$ is also a function of ρ, according to Eq. (23), and the matrix elements in Eq. (28) may be readily integrated.

Evaluation of the real level shift is more complicated since

$$\Delta_{ij}(E) = \sum_{\nu}\frac{1}{2\pi}p\int dE' \times\frac{\langle\eta_i|\Gamma^{1/2}(E'-\varepsilon_\nu)|\eta_\nu\rangle\langle\eta_\nu|\Gamma^{1/2}(E'-\varepsilon_\nu)|\eta_j\rangle}{E-E'}, \tag{29}$$

and we do not know the energy integral in closed form. The simplest way to integrate Eq. (29) is neglecting the dependence of $\Gamma(E-\varepsilon_\nu)$ on the vibrational quantum number and applying the closure relation of the vibrational eigenstates, since the integral of $\Gamma(E)/(E-E')$ is given by Eq. (24). Though this local approximation would in principle be inadequate for near threshold collisions ($E\sim\varepsilon_\nu$), it could be legitimate if the width was weakly dependent on the vibrational coordinate,

$$\Gamma_{ij}(E) \simeq \Gamma(E,0)\delta_{ij} \Rightarrow \Delta_{ij}(E) = \Delta(E,0)\delta_{ij}, \tag{30}$$

where $\rho=0$ is the equilibrium geometry and δ_{ij} is the Kronecker delta, or, alternatively,

$$\Gamma_{ij}(E) \simeq \langle\eta_i|\Gamma(E-\bar{\varepsilon})|\eta_j\rangle \Rightarrow \Delta_{ij}(E) = \langle\eta_i|\Delta(E-\bar{\varepsilon})|\eta_j\rangle, \tag{31}$$

with some suitable choice of $\bar{\varepsilon}$. We will refer to Eqs. (30) and (31) as Condon and local approximations for the level shift, respectively (though, strictly, both are local approximations). The width matrix elements are always calculated as in Eq. (28), thus keeping the nonlocal and energy-dependent character, and the present local approximation for the level shift should not be confused with the local approximation ("boomerang model") defined elsewhere [53,55]; our definition is similar to the semilocal approximation of Cederbaum and Domcke [73], and to the approach of Hazi *et al.* [74]. It would be instructive to compare these simpler approximations for Δ with the fully nonlocal approach since the former might be of help in applications to larger molecules.

Though we cannot take an advantage from Eq. (24) without a local assumption, we know the integrand of Eq. (29) in closed form and the numerical evaluation of $\Delta_{ij}(E)$ on an energy quadrature would not be difficult. The matrix elements in Eq. (29) could be performed as previously described for the widths: once the model parameters are obtained from least-squares fits to SMC eigenphases on quadrature points, integration over ρ may be readily carried out with the help of Eq. (23). An analytical expression for the nonlocal level shift has been obtained [57] by describing the target potential surface with a Morse oscillator and assuming a separable form for the width, $\Gamma(E;\rho)=g(E)h(\rho)$, with different sets of model parameters for the functions g and h. Though this procedure would simplify the calculation, we prefer the (nonlocal) evaluation of Δ_{ij} on an energy quadrature since the underlying numerical effort for one dimensional systems (those with a single vibrational mode) does not challenge the current computational capabilities, and the extension to multidimensional systems would be straightforward. For completeness, we explicitly write the working expression for the vibrational excitation cross section (omitting the background term),

$$\sigma_{\nu_i\to\nu_f} = \frac{2\pi}{E}\left|\sum_{\nu\mu}\Gamma^{1/2}_{f\mu}(E_f)[\mathcal{D}^{-1}]_{\mu\nu}\Gamma^{1/2}_{\nu i}(E)\right|^2, \tag{32}$$

where

$$\mathcal{D}_{\mu\nu} = \langle\eta_\mu|[E-K-V_{\rm opt}(E-\tilde{H}_N)]|\eta_\nu\rangle. \tag{33}$$

III. COMPUTATIONAL PROCEDURES

A. Fixed-nuclei calculations

The Cartesian Gaussian basis set used in fixed-nuclei calculations is given elsewhere [34]. The target electronic ground state was described at the restricted Hartree-Fock (HF) level with a $7s4p$ basis set augmented with a p-type function at the center of mass, and the scattering basis set

was further augmented with p-type functions on dummy centers located at the corners of a cube. The equilibrium interatomic distance $d_{eq}=1.387a_0$ was obtained from geometry optimization with the HF potential [75], and the corresponding harmonic frequency was $\hbar\omega=0.569$ eV (the respective experimental values are $1.401a_0$ [76] and 0.545 eV [77]). Scattering calculations were performed for $d=0.658a_0$, $0.869a_0$, $1.051a_0$, $1.221a_0$, $1.387a_0$, $1.552a_0$, $1.722a_0$, $1.904a_0$, and $2.115a_0$, where $\rho=(d-d_{eq})$, and polarization effects (target distortion due to the interaction with the positron) were accounted for by including all singly excited target states in the closed-channel (Q) space. A Koopman's theorem estimate of the ionization potential yields the positronium formation threshold $E_{Ps}=9.38$ eV in our model, lying 0.8 eV above the experimental value, $E_{Ps}=8.6$ eV. Since we focus on low energy collisions ($E\leq 3$ eV), the positronium formation channel could be safely neglected.

B. Vibrational excitation calculations

The operators and wave functions were represented on an evenly spaced 128-point grid ranging from $0.5a_0$ to $4.5a_0$. The set of model parameters $\{a,A,b,\epsilon_d\}$ was interpolated for $0.658a_0\leq d\leq 2.115a_0$ and linearly extrapolated to the lower and upper ends of the numerical grid. These regions not covered by scattering calculations were only necessary to represent highly excited vibrational eigenstates and the $0\rightarrow 0,1,2$ excitation cross sections were insensitive to the extrapolation scheme.

The target vibrational eigenstates were obtained from the benchmark potential energy surface of Kolos and Wolniewicz [78] employing the energy screening technique [79], and the $0\rightarrow 0,1,2$ cross sections were well converged with the representation of the nonlocal operator truncated at $\nu=8$. The energy integration in Eq. (29) was performed with $(2N)$-point Gauss-Legendre quadratures, where N points were employed for each of the $(0\leq E'<E)$ and $(E<E'<\infty)$ intervals, and numerical convergence was obtained with $N=22$.

IV. RESULTS AND DISCUSSION

A. Fixed-nuclei calculations

The eigenphase sum in Eq. (21) can be approximated by a single partial wave in case the latter dominates the cross section in the energy range of interest (typically, in the vicinity of a resonance). In the present case, we are interested in the low energy limit ($E\rightarrow 0$) of fixed-nuclei eigenphase sums, as they ultimately determine the behavior of the widths $\Gamma(E_f)$ and cross sections in near threshold ($E_f\simeq 0$) vibrationally inelastic collisions. It is thus legitimate to approximate the eigenphase sum by the s wave phase shift at low energies, as it accounts for over 95% of the fixed-nuclei cross sections at 0.5 eV and for about 80% at 1 eV (as shown below, the relevant threshold effects are seen around $0<E_f<0.5$ eV).

The s wave phase shifts obtained from fixed-nuclei SMC calculations and the corresponding least-squares fits are shown in Fig. 1 for the interatomic distances given in Sec. III A. It is easy to keep track of the parametric dependence on ρ since the peak heights around 0.50 eV increase monotonically with the interatomic distance. Despite the simplicity of Eqs. (23) and (25), the model provides a good description of the eigenphase over the fairly broad energy range $0\leq E\leq 4$ eV, though a better agreement with SMC data is seen for $E\leq 3$ eV. Below 3 eV, the average deviation of the least-squares fit from calculated SMC points (all energies and interatomic distances) was 2%, and the maximum deviation did not exceed 6%. Since the model faithfully describes the s wave phase shifts beyond 1 eV, it can be combined with $l\geq 1$ partial waves obtained with the ANV approximation to vibrationally resolve the collisions at higher energies. (Alternatively, one could augment the model with higher order $E^{(l+1)/2}$ terms and perform least-squares fits to the SMC eigenphase sum.) The corresponding level shifts (Δ) and widths (Γ) are shown in Fig. 2, where the dependence on ρ may be easily followed: the width peak heights ($\sim$0.70 eV)

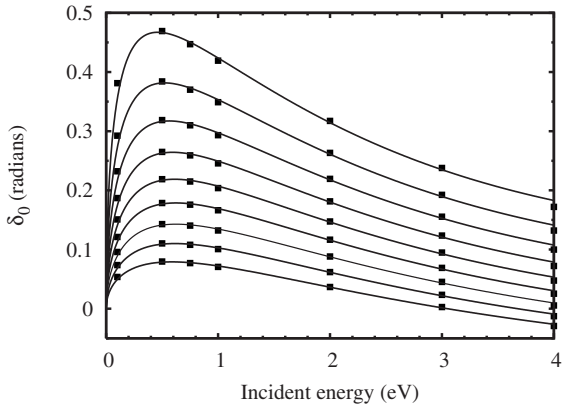

FIG. 1. Fixed-nuclei s wave scattering phase shifts (δ_0) for the interatomic distances given in Sec. III A (peak heights around 0.50 eV monotonically increase with the interatomic distance). The lines are least-squares fits to the SMC calculations (squares).

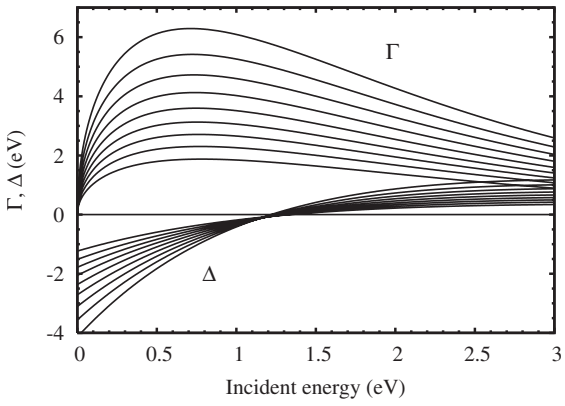

FIG. 2. Fixed-nuclei level shifts (Δ) and widths (Γ) for the interatomic distances given in Sec. III A. The peak heights of Γ around 0.70 eV monotonically increase with the interatomic distance, while the level shift values at zero energy are monotonically decreasing (the latter trend is inverted at higher energies due to the crossings around 1.2 eV).

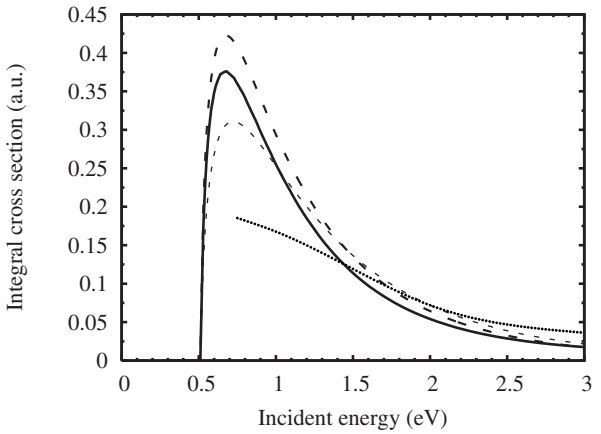

FIG. 3. S wave partial cross section for the $0\rightarrow1$ vibrational excitation of H_2 by positron impact. Dotted line: ANV result of Refs. [31,32]; thin dashed line: Condon approximation for the level shift; thick dashed line: local approximation for the level shift; solid line: full nonlocal calculation.

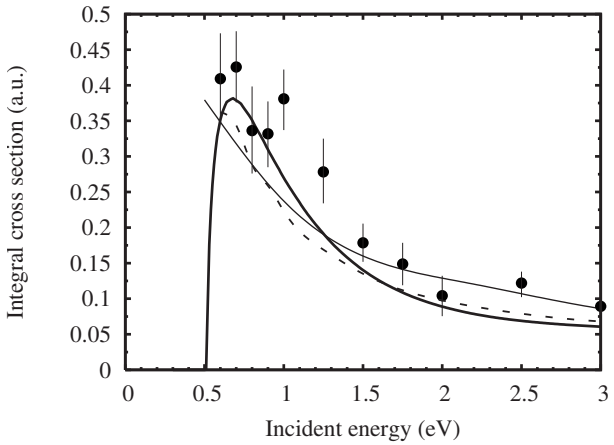

FIG. 4. Integral cross section for the $0\rightarrow1$ vibrational excitation of H_2 by positron impact. Thick solid line: present result; thin solid line: theory of Sur and Ghosh [81]; dashed line: theory of Gianturco and Mukherjee [24] (corrected results of Ref. [23]); circles: experimental data of Sullivan *et al.* [4].

increase monotonically with the interatomic distance, while the level shift values at zero energy are monotonically decreasing (the latter trend is inverted at higher energies due to the crossings around 1.2 eV).

The $\mathcal{Q}$-$\mathcal{P}$ decomposition of the scattering wave function gives rise to the decomposition of the eigenphase into background and singular (Breit-Wigner) terms, according to Eqs. (21) and (22). The position of the singularities in the complex momentum plane is given by the corresponding fixed-nuclei complex potentials $(\epsilon_d,\Delta,\Gamma)$, so the essential information obtained from the fits of the model to SMC eigenphases is where to locate the singularities in the complex k plane. Though positrons are known to form virtual and weakly bound states with molecules, our model does not describe such low lying singularities [80]; the scattering lengths, $\alpha=-\lim_{k\rightarrow0}\delta_0(k)/k$, ranged from $-3.578a_0$ to $-0.444a_0$, monotonically increasing in magnitude with ρ, where $\alpha_{eq}=-1.291a_0$. For the interatomic distances of interest, the fits over $0<E<4$ eV gave rise to high lying (>8.5 eV) narrow resonances not overlapping the threshold, so the low energy behavior of the eigenphase could be viewed as the "nonsingular" limit of the model (as opposed to the "singular" limit that would arise from sharp low lying singularities). It can be inferred from Fig. 2 that the widths are small beyond 8 eV (actual values do not exceed 0.1 eV), and by noting that $[E-\epsilon_d-\Delta(E)]\simeq\epsilon_d$ for $E\simeq\Delta(E)\ll\epsilon_d$, we obtain $\delta_d(E)\simeq-\tan[\Gamma(E)/2\epsilon_d]$ from Eq. (22). This smooth discrete component eigenphase was still dominant at low energies $(\delta_0\simeq\delta_d)$, since the peak shaped eigenphases in Fig. 1 could not be described with the simple threshold expansion assumed for the background, Eq. (25). Though the energy dependence of the eigenphase (Fig. 1) and complex potential (Fig. 2) does not arise from low lying virtual or bound states, it is not trivial in the sense that the vibrational excitation cannot be properly described with the ANV approximation (see below), suitable for low energy e^--H_2 scattering [31,32].

B. Vibrational excitation cross sections

The s wave dominates the near-threshold scattering, and its contribution to the $0\rightarrow1$ excitation cross section, obtained with different approximations for the level shift, is shown in Fig. 3. The s wave background was calculated with the ANV approximation, and its contribution to vibrationally inelastic scattering was modest, as expected (about 10% of the $0\rightarrow1$ cross section). Though discrepancies around 25% are seen at the peaks, there is good agreement among Condon (thin dashed line), local (thick dashed line), and nonlocal (solid line) calculations, where $\bar{\varepsilon}=(\varepsilon_i+\varepsilon_j)/2$ was employed in the local approximation [see Eq. (31)]. The ANV result of Refs. [31,32] is rather poor below 1.5 eV, as expected, since the adiabatic T matrix does not have the correct energy dependence at threshold. Though a proper description of the dependence on the vibrational coordinate should be important in case virtual or bound states are found, Fig. 3 suggests that meaningful results may be obtained with computationally inexpensive approximations for the level shift, and these might be helpful to describe more challenging systems having more than a single vibrational mode.

The $0\rightarrow1$ integral cross section is shown in Fig. 4 (thick solid line), where the s and higher partial waves $(l=1,2)$ were obtained with the nonlocal and ANV [31,32] schemes, respectively (the s wave background was also accounted for with the ANV approximation). Our results compare favorably with the experimental data of Sullivan *et al.* [4], especially at lower energies, and once more indicate that properly describing the threshold energy dependence is essential. In general, there is also agreement with the theory of Sur and Ghosh [81] and with the corrected result [24] of Gianturco and Mukherjee [23]. The local description of the level shift (thick dashed line in Fig. 3) provides an even better agreement with experimental data, but this is of course fortuitous (compensation among errors). The discrepancy between ANV and nonlocal calculations (Fig. 3) is not trivial in the sense that the adiabatic $0\rightarrow1$ excitation cross section by

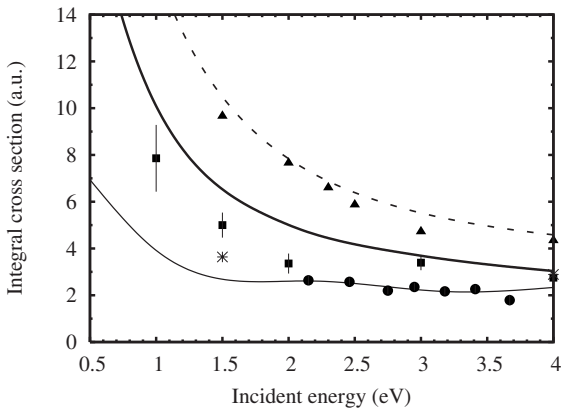

FIG. 5. Total cross section for positron scattering by H_2. Thick solid line: present result; thin solid line: theory of Sur and Ghosh [81]; dashed line: theory of Gianturco and Mukherjee [24] (corrected results of Ref. [23]); triangles: experimental data of Karwasz *et al.* [82]; circles: experimental data of Charlton *et al.* [83]; squares: experimental data of Hoffman *et al.* [84]; stars: experimental data of Zhou *et al.* [85].

electron impact is quite reasonable at low energies [31,32]. Though virtual states were not found (see Sec. IV A), the (fixed-nuclei) elastic positron scattering cross section has a sharp slope at low energies not seen in the electron case [31,32,34], and the resulting energy dependence of the vibrational excitation cross section cannot be accounted for in the ANV picture. In this sense, the e^+-H_2 system could be viewed as on the way of forming a virtual state.

For completeness, the total cross section (TCS) is shown in Fig. 5 as the sum of the $0\rightarrow 0,1$ cross sections ($\sigma_{0\rightarrow 2} < 10^{-3} a_0^2$), where the s wave background and the $l=1,2$ partial waves were described with the ANV approximation. Despite the good agreement between theory and experiment for the $0\rightarrow 1$ excitation cross section (Fig. 4), a puzzling disagreement is seen in the TCS. It would be difficult to point out the best experimental data, and the need of further TCS measurements for e^+-H_2 collisions was recently stressed by Karwasz and co-workers [82]. At low energies, their results are above the experimental data of other groups also for argon and nitrogen, though in good agreement with the calculations of Gianturco and Mukherjee for hydrogen (corrected results of Ref. [24]). The theory of Sur and Ghosh [81] agrees very well with the measurements of Charlton *et al.* [83] above 2 eV, and the present results compare favorably with the experimental data of Hoffman *et al.* [84] (the TCS of Zhou *et al.* [85] at 1.5 eV lies below the result of Ref. [84]). We believe the discrepancies among the theories could arise from the low energy behavior of the vibrationally elastic cross sections. In this case, the disagreement would be more closely related to the description of the (fixed-nuclei) scattering polarization potentials than to the vibrational resolution schemes.

V. CONCLUSIONS

We have reported vibrational excitation cross sections for positron scattering by H_2 obtained with the Feshbach projection-operator formalism and SMC fixed-nuclei calculations. The projection-operator approach has long been a powerful tool for studies of nuclear dynamics in electron-molecule collisions, and its application to positron scattering is timely since couplings to nuclear degrees of freedom are known to be important at low impact energies. Though our fixed-nuclei calculations do not support the existence of a e^+-H_2 virtual state, the good agreement between the calculated $0\rightarrow 1$ excitation cross section with experimental data near the threshold, where adiabatic excitation results are poor, arises from a proper description of the T matrix energy dependence.

We believe the combination of *ab initio* fixed-nuclei calculations with the projection operator formalism is a promising framework for studies of vibrationally resolved positron scattering at low energies. Exploratory calculations for acetylene (to be published) show a rich dynamics with dramatic threshold effects in the excitation of symmetry-preserving (infrared inactive) vibrational modes, similar to those recently reported by Franz and Gianturco [29].

ACKNOWLEDGMENTS

M.A.P.L. acknowledges support from the Brazilian agency Conselho Nacional de Desenvolvimento Científico e Tecnológico (CNPq). The calculations presented here were partly performed at Centro Nacional de Processamento de Alto Desempenho (CENAPAD-SP).

[1] S. J. Gilbert, C. Kurz, R. G. Greaves, and C. M. Surko, Appl. Phys. Lett. **70**, 1944 (1997).
[2] S. J. Gilbert, R. G. Greaves, and C. M. Surko, Phys. Rev. Lett. **82**, 5032 (1999).
[3] S. J. Gilbert, J. Sullivan, R. G. Greaves, and C. M. Surko, Nucl. Instrum. Methods Phys. Res. B **171**, 81 (2000).
[4] J. P. Sullivan, S. J. Gilbert, and C. M. Surko, Phys. Rev. Lett. **86**, 1494 (2001).
[5] J. P. Sullivan, S. J. Gilbert, S. J. Buckman, and C. M. Surko, J. Phys. B **34**, L467 (2001).
[6] J. P. Sullivan, J. P. Marler, S. J. Gilbert, S. J. Buckman, and C. M. Surko, Phys. Rev. Lett. **87**, 073201 (2001).
[7] J. P. Marler, J. P. Sullivan, and C. M. Surko, Phys. Rev. A **71**, 022701 (2005).
[8] J. P. Marler and C. M. Surko, Phys. Rev. A **72**, 062713 (2005).
[9] J. P. Marler and C. M. Surko, Phys. Rev. A **72**, 062702 (2005).
[10] S. J. Gilbert, L. D. Barnes, J. P. Sullivan, and C. M. Surko, Phys. Rev. Lett. **88**, 043201 (2002).
[11] L. D. Barnes, S. J. Gilbert, and C. M. Surko, Phys. Rev. A **67**, 032706 (2003).
[12] L. D. Barnes, J. A. Young, and C. M. Surko, Phys. Rev. A **74**, 012706 (2006).

[13] G. F. Gribakin and P. M. W. Gill, Nucl. Instrum. Methods Phys. Res. B **221**, 30 (2004).
[14] J. P. Marler, G. F. Gribakin, and C. M. Surko, Nucl. Instrum. Methods Phys. Res. B **247**, 87 (2006).
[15] G. F. Gribakin and C. M. R. Lee, Phys. Rev. Lett. **97**, 193201 (2006).
[16] G. F. Gribakin, Nucl. Instrum. Methods Phys. Res. B **192**, 26 (2002); G. F. Gribakin and C. M. R. Lee, *ibid.* **247**, 31 (2006).
[17] G. F. Gribakin, Phys. Rev. A **61**, 022720 (2000).
[18] K. Iwata, G. F. Gribakin, R. G. Greaves, C. Kurz, and C. M. Surko, Phys. Rev. A **61**, 022719 (2000).
[19] K. Iwata, R. G. Greaves, T. J. Murphy, M. D. Tinkle, and C. M. Surko, Phys. Rev. A **51**, 473 (1995).
[20] K. Iwata, R. G. Greaves, and C. M. Surko, Phys. Rev. A **55**, 3586 (1997).
[21] F. A. Gianturco and T. Mukherjee, Europhys. Lett. **48**, 519 (1999); Eur. Phys. J. D **7**, 211 (1999).
[22] F. A. Gianturco and T. Mukherjee, Nucl. Instrum. Methods Phys. Res. B **171**, 17 (2000).
[23] F. A. Gianturco and T. Mukherjee, Phys. Rev. A **55**, 1044 (1997).
[24] F. A. Gianturco and T. Mukherjee, Phys. Rev. A **64**, 024703 (2001).
[25] T. Nishimura and F. A. Gianturco, Nucl. Instrum. Methods Phys. Res. B **192**, 17 (2002); Phys. Rev. A **65**, 062703 (2002); Europhys. Lett. **59**, 674 (2002).
[26] T. Nishimura and F. A. Gianturco, Phys. Rev. Lett. **90**, 183201 (2003).
[27] T. Nishimura and F. A. Gianturco, Nucl. Instrum. Methods Phys. Res. B **221**, 24 (2004); Europhys. Lett. **68**, 377 (2004).
[28] T. Nishimura and F. A. Gianturco, Phys. Rev. A **72**, 022706 (2005); Eur. Phys. J. D **33**, 221 (2005).
[29] F. A. Gianturco, J. Franz, R. J. Buenker, H.-P. Liebermann, L. Pichl, J.-M. Rost, M. Tachikawa, and M. Kimura, Phys. Rev. A **73**, 022705 (2006); J. Franz and F. A. Gianturco, Nucl. Instrum. Methods Phys. Res. B **247**, 20 (2006); Eur. Phys. J. D **39**, 407 (2006).
[30] E. P. da Silva, J. S. E. Germano, J. L. S. Lino, C. R. C. de Carvalho, Alexandra P. P. Natalense, and Marco A. P. Lima, Nucl. Instrum. Methods Phys. Res. B **143**, 140 (1998).
[31] F. Arretche, R. F da Costa, S. d'A. Sanchez, A. N. S. Hisi, E. M. de Oliveira, M. T. do N. Varella, and M. A. P. Lima, Nucl. Instrum. Methods Phys. Res. B **247**, 13 (2006).
[32] A. N. S. Hisi, M.S. Dissertation, Physics Institute, State University of Campinas (UNICAMP), Campinas, 2006 (in Portuguese).
[33] E. P. da Silva, J. S. E. Germano, and Marco A. P. Lima, Phys. Rev. Lett. **77**, 1028 (1996).
[34] J. L. S. Lino, J. S. E. Germano, E. P. da Silva, and M. A. P. Lima, Phys. Rev. A **58**, 3502 (1998).
[35] C. R. C. de Carvalho, M. T. do N. Varella, E. P. da Silva, J. S. E. Germano, and M. A. P. Lima, Nucl. Instrum. Methods Phys. Res. B **171**, 33 (2000).
[36] M. T. do N. Varella, C. R. C. de Carvalho, M. A. P. Lima, and E. P. da Silva, Phys. Rev. A **63**, 052705 (2001).
[37] M. T. do N. Varella, C. R. C. de Carvalho, and M. A. P. Lima, Nucl. Instrum. Methods Phys. Res. B **192**, 225 (2002).
[38] C. R. C. de Carvalho, M. T. do N. Varella, M. A. P. Lima, and E. P. da Silva, Phys. Rev. A **68**, 062706 (2003).
[39] S. d'A. Sanchez, F. Arretche, M. T. do N. Varella, and M. A. P. Lima, Phys. Scr. **T110**, 276 (2004).
[40] P. Chaudhuri, M. T. do N. Varella, C. R. C. de Carvalho, and M. A. P. Lima, Nucl. Instrum. Methods Phys. Res. B **221**, 69 (2004); Phys. Rev. A **69**, 042703 (2004).
[41] E. P. da Silva, M. T. do N. Varella, and M. A. P. Lima, Phys. Rev. A **72**, 062715 (2005).
[42] H. Feshbach, Ann. Phys. (N.Y.) **5**, 357 (1958); **19**, 287 (1962).
[43] W. Domcke, Phys. Rep. **208**, 97 (1991).
[44] M. Čížek, M. Thoss, and W. Domcke, Phys. Rev. B **70**, 125406 (2004); C. Benesch, M. Čížek, M. Thoss, and W. Domcke, Chem. Phys. Lett. **430**, 355 (2006); J. Horáček, M. Čížek, K. Houfek, P. Kolorenč, and W. Domcke, Phys. Rev. A **73**, 022701 (2006).
[45] C. W. McCurdy, W. A. Isaacs, H.-D. Meyer, and T. N. Rescigno, Phys. Rev. A **67**, 042708 (2003); W. Vanroose, Z. Zhang, C. W. McCurdy, and T. N. Rescigno, Phys. Rev. Lett. **92**, 053201 (2004); D. J. Haxton, Z. Zhang, H.-D. Meyer, T. N. Rescigno, and C. W. McCurdy, Phys. Rev. A **69**, 062714 (2004); D. J. Haxton, C. W. McCurdy, and T. N. Rescigno, *ibid.* **73**, 062724 (2006).
[46] M. Born and J. R. Oppenheimer, Ann. Phys. (Leipzig) **84**, 457 (1927).
[47] D. M. Chase, Phys. Rev. **104**, 838 (1956).
[48] E. P. Wigner, Phys. Rev. **73**, 1002 (1948).
[49] J. S. E. Germano and M. A. P. Lima, Phys. Rev. A **47**, 3976 (1993).
[50] J. C. Y. Chen, Phys. Rev. **148**, 66 (1966).
[51] T. F. O'Malley, Phys. Rev. **150**, 14 (1966).
[52] J. N. Bardsley, J. Phys. B **1**, 349 (1968).
[53] L. Dubé and A. Herzenberg, Phys. Rev. A **20**, 194 (1979).
[54] W. Domcke and L. S. Cederbaum, Phys. Rev. A **16**, 1465 (1977).
[55] A. U. Hazi, T. N. Rescigno, and M. Kurilla, Phys. Rev. A **23**, 1089 (1981).
[56] The BO approximation is expected to be valid for the discrete state since the typical separation between resonant states is of the same order of magnitude as the separation of molecular electronic states (the key BO assumption is a separation between electronic levels that largely exceeds the separation of vibrational levels [46]).
[57] M. Berman, H. Estrada, L. S. Cederbaum, and W. Domcke, Phys. Rev. A **28**, 1363 (1983).
[58] C. J. Joachain, *Quantum Collision Theory* (North-Holland, Amsterdam, 1975).
[59] A formal solution of the background problem is discussed elsewhere [51]. Here we assume the ANV approximation is legitimate in the $\mathcal{P}$ space.
[60] W. Domcke, J. Phys. B **14**, 4889 (1981).
[61] Though we usually employ $N(k)=1$ in SMC calculations [49], $N(k)=\sqrt{m_e k/\hbar^2(2\pi)^3}$ (atomic units, $\hbar=m_e=1$, are used in the text) is more convenient for definition of the width Γ. The normalization convention is not important in practice, since s wave eigenphases are the fixed-nuclei input in the vibrational excitation T matrix (see Sec. II B 1).
[62] J. N. Bardsley, A. Herzenberg, and F. Mandl, Proc. Phys. Soc. London **89**, 305 (1966).
[63] A. U. Hazi and H. S. Taylor, Phys. Rev. A **1**, 1109 (1970).
[64] A. U. Hazi, in *Electron-Molecule and Photon-Molecule Collisions*, edited by T. N. Rescigno, V. McKoy, and B. I. Schneider

(Plenum, New York, 1979).
[65] U. V. Riss and H.-D. Meyer, J. Phys. B **26**, 4503 (1993).
[66] P. Kolorenč, V. Brems, and J. Horáček, Phys. Rev. A **72**, 012708 (2005); B. M. Nestman, J. Phys. B **31**, 3929 (1998).
[67] H. Estrada and W. Domcke, J. Phys. B **18**, 4469 (1985).
[68] J. Tennyson and C. J. Noble, Comput. Phys. Commun. **33**, 421 (1984); D. T. Stibbe and J. Tennyson, Phys. Rev. Lett. **79**, 4116 (1997).
[69] A. U. Hazi, Phys. Rev. A **19**, 920 (1979).
[70] M. Berman and W. Domcke, Phys. Rev. A **29**, 2485 (1984).
[71] M. Abramowitz and I. A. Stegun, *Handbook of Mathematical Functions* (Dover, New York, 1965).
[72] As pointed out by Hazi *et al.* [55], the phase of the entry (exit) amplitude can be viewed as weakly dependent on the vibrational coordinate and does not contribute to vibrationally resolved cross sections; in practice, it is often assumed real (see Refs. [45,55,57,67]).
[73] L. S. Cederbaum and W. Domcke, J. Phys. B **14**, 4665 (1981).
[74] A. U. Hazi, A. E. Orel, and T. N. Rescigno, Phys. Rev. Lett. **46**, 918 (1981).
[75] GAMESS package: M. W. Schmidt, K. K. Baldridge, J. A. Boatz, S. T. Elbert, M. S. Gordon, J. H. Jensen, S. Koseki, N. Matsunaga, K. A. Nguyen, S. J. Su, T. L. Windus, M. Dupuis, and J. A. Montgomery, J. Comput. Chem. **14**, 1347 (1993).
[76] *CRC Handbook of Chemistry and Physics*, edited by R. C. Weast, 69th ed. (CRC Press, Boca Raton, 1988).
[77] K. P. Huber and G. Herzberg, *Molecular Spectra and Molecular Structure. IV. Constants of Diatomic Molecules* (Van Nostrand Reinhold, New York, 1979).
[78] W. Kolos and L. Wolniewicz, J. Chem. Phys. **43**, 2429 (1965).
[79] K. Takatsuka and N. Hashimoto, J. Chem. Phys. **103**, 6057 (1995).
[80] The analytical properties of the S matrix and eigenphases can be readily surveyed with the help of Eqs. (23) and (24), as discussed elsewhere [60,67]. The positions of the singularities (E_s) are given by $E_s-\epsilon_d-\Delta(E_s)=0$, according to Eq. (22), and the corresponding widths are $\Gamma(E_s)$. Bound and virtual states correspond to singularities on the imaginary k axis ($\Gamma=0$), while resonances give rise to singularities off the imaginary axis [58].
[81] S. Sur and A. S. Ghosh, J. Phys. B **18**, L715 (1985).
[82] G. Karwasz, D. Pliszka, and R. S. Brusa, Nucl. Instrum. Methods Phys. Res. B **247**, 68 (2006).
[83] M. Charlton, T. C. Griffith, G. R. Heyland, and G. L. Wright, J. Phys. B **16**, 323 (1983).
[84] K. R. Hoffman, M. S. Dababneh, Y.-F. Hsieh, W. E. Kauppila, V. Pol, J. H. Smart, and T. S. Stein, Phys. Rev. A **25**, 1393 (1982).
[85] S. Zhou, H. Li, W. E. Kauppila, C. K. Kwan, and T. S. Stein, Phys. Rev. A **55**, 361 (1997).